

Volatile Metabolomics from Cashew Leaves: Assessment of Resistance Biomarkers Associated with Black Mold (*Pilgeriella anacardii* Arx & Müller)

Debora B. de Sousa,^a Gisele S. da Silva,^{id b} Jhonyson A. C. Guedes,^{id a,b} Luiz A. L. Serrano,^b Marlon V. V. Martins,^b Tigressa H. S. Rodrigues,^{id c} Edy S. de Brito,^{id b} Davila Zampieri,^a Mary A. S. Lima^{id a} and Guilherme J. Zocolo^{id *,b}

^aDepartamento de Química Orgânica e Inorgânica, Universidade Federal do Ceará, 60440-900 Fortaleza-CE, Brazil

^bEmbrapa Agroindústria Tropical, 60511-110 Fortaleza-CE, Brazil

^cCurso de Química, Centro de Ciências e Tecnologia, Universidade Vale do Acaraú, 62040-370 Sobral-CE, Brazil

Black mold, a disease caused by the fungus *Pilgeriella anacardii* Arx & Müller, affects cashews (*Anacardium occidentale*). Some cashew clones are more resistant to the pathogen; however, little is known about the chemical profile responsible for this trait. The investigation of volatile organic compounds (VOCs) from leaves of dwarf cashew clones resistant (BRS 226 and BRS 265) and susceptible (CCP 76 and BRS 189) to the pathogen was carried out. Leaves were collected during the months of disease incidence and decline (March to July 2019, Brazil), and VOCs were analyzed by gas chromatography-mass spectrometry (GC-MS) combined with chemometric tools. The GC-MS analysis tentatively identified 96 compounds. Partial least squares discriminant analysis (PLS-DA), orthogonal partial least squares discriminant analysis (OPLS-DA), hierarchical cluster analysis (HCA), and ROC curves analysis were useful in dividing VOCs into distinct resistance and associated chemical susceptibility groups for different clones. The VOCs in the leaves of the resistant clones were identified as alcohols and aldehydes containing six carbons: (*E*)-hex-2-enal, hex-3-en-1-ol, (*Z*)-hex-2-en-1-ol, (*E*)-hex-2-en-1-ol, and hexan-1-ol. Moreover, α -pinene, pseudolimonene, α -phellandrene, β -myrcene, sylvestrene, β -*cis*-ocimene, methyl salicylate, myrtenol, α -copaene, γ -muurolene, germacrene D, valencene, and germacrene B were also detected in these samples and may be candidate chemical biomarkers for cashew resistance to *P. anacardii*.

Keywords: *Anacardium occidentale*, resistance, susceptibility, *Pilgeriella anacardii*, chemometric analysis, biomarkers

Introduction

The cashew tree (*Anacardium occidentale* L.) is a plant originally from Brazil that is cultivated with great importance in the semi-arid region of the country, occupying approximately 500 thousand hectares. Its main product is cashew nut, an important commodity that generates approximately US\$ 100 million *per year* for the country. The world's largest consumers of cashew nuts are India, the United States, and the European Union.¹

Common cashew trees are large plants with a height that can exceed 10 m, which makes manual harvesting impossible with consequent loss of cashew pulp. To

maximize the use of cashew products, from the 1980s onwards Brazil consolidated a strong genetic improvement program, resulting in the provision of 12 clonal genotypes, 10 of which are called dwarf-cashew (height less than 4 m). Dwarf-cashew clones allow manual harvesting of fruits, increasing the use and quality of cashew nuts and pulps, and favor the achievement of more productive orchards.²

However, some cultivars of dwarf-cashew clones have suffered severe attacks of a black mold, which is caused by the phytopathogen *Pilgeriella anacardii* Arx & Müller.³ This fungus is characterized by being an obligatory parasite that colonizes the lower part of the mature leaves of the cashew tree, where it is possible to observe the formation of a layer of black mycelium.⁴ The first symptom of the disease is the occurrence of spots indicative of insufficiency in the production of chlorophyll, which results in the yellowing

*e-mail: guilherme.zocolo@embrapa.br

Editor handled this article: Eduardo Carasek

of the leaves at the beginning of the rainy season. This disease is highly disseminated in orchards that produce cashews in May, just after two months of intense rain in the semi-arid region.⁴

Owing to the lack of fungicides registered to control black mold disease in cashew cultivars, the use of genetic resistance presented by some clones has been reported as an efficient and economically viable alternative for the implantation of orchards.⁵ Besides, the understanding of the chemical compound profile related to this resistance may favor the cashew clone breeding program in the search for new genotypes with resistance to diseases, as well as for the development of biopesticidal organic compounds.

The literature reports that when plants are under attack by pathogenic microorganisms, they biosynthesize volatile organic compounds (VOCs) that have antibacterial, antifungal, and antioxidant functions as signs of defense responses. Thus, metabolomic studies are frequently performed to identify the mechanisms related to plant-pathogen interactions.^{6,7}

The dwarf-cashew clones BRS 265 and BRS 226 were resistant to the attack of the *P. anacardii*, whereas BRS 189 and CCP 76 were susceptible to black mold disease.⁸ According to these results, this work reports the investigation of the chemical profile of VOCs emitted from leaves of resistant and susceptible dwarf-cashew clones in response to the incidence and decline of black mold disease. The VOCs were analyzed by gas chromatography-mass spectrometry (GC-MS), and the spectral data were interpreted using chemometric tools to identify possible chemical biomarkers.

Experimental

Plant material

The leaves of the cashew clones CCP 76, BRS 226, BRS 189, and BRS 265 were collected at the Embrapa Agroindústria Tropical (Experimental Field), located in the municipality of Pacajus, Ceará State, Brazil (geographical coordinates of the place: 4°10'S and 38°27'W and altitude of 60 m above sea level). The orchard of these clone types of dwarf cashews was planted in May 2011 under a rainfed regime. Since implantation, the orchard has received all the cultural treatments recommended by Serrano and de Oliveira.⁹ Agrochemicals with probable action on black mold were not applied to the area.

Sample collection was conducted from March to July 2019, with one collection *per* month. From each of the four types of clones evaluated, five plants were selected, from which three leaves of the same size

(approximately 9 cm) were collected, totaling 60 samples *per* collection. Leaf samples collected in March did not show disease symptoms for any clone type. The leaf samples collected in April and May showed features associated with symptoms of the disease for clones CCP 76 and BRS 189. In June and July, no leaf samples showed symptoms of the disease. Fresh leaf samples were collected in the morning period. The samples were placed inside 20 mL vials with screw caps containing silicone septum/polytetrafluoroethylene (PTFE) (Supelco, Bellefonte, PA, USA), specific for analysis using GC-MS. After collection, the vials containing the samples were placed inside a Styrofoam box containing an ice bath until GC-MS analysis was carried out in triplicate.

Extraction and analysis of the volatile organic compounds

Solid-phase microextraction (SPME) using the headspace technique was used to extract volatile compounds from the leaves of each investigated cashew clone. The experimental conditions for SPME analyses were according to Rouseff *et al.*¹⁰ The vials containing the samples were pre-incubated at 30 °C for 30 min without shaking, and a divinylbenzene/carboxen/polydimethylsiloxane (DVB/CAR/PDMS) gray fiber of 1 cm (Supelco, Bellefonte, PA, USA) was exposed inside the vials for the adsorption of volatile compounds for 15 min in the headspace. After the extraction time, the fiber was removed from the vials and sent to the gas chromatograph injector, where it remained for 3 min for thermal desorption (at 260 °C) of the captured analytes. The elution of the compounds through the column occurred with temperature variation, and the initial column temperature was maintained at 40 °C and programmed to 260 °C at a rate of 7 °C min⁻¹.

The gas chromatograph used in the analysis was a 7890B GC System from Agilent Technologies Spain (Madrid, Spain) coupled to a mass spectrometer with a quadrupole analyzer (5977A MSD Agilent Technologies Spain). The column used was HP5-MS ((5%-phenyl)-dimethylpolysiloxane) with an internal diameter of 30 m × 0.25 mm internal diameter and a film thickness of 0.25 µm. The analyses were performed in splitless mode, using helium gas as the carrier of the analytes, at a flow rate of 1 mL min⁻¹.

To obtain the mass spectra, electron impact ionization at 70 eV was used, with a mass range of 50-600 Da. The temperature used in the transfer line was 280 °C and the ionization source was 150 °C. The identification of the obtained compounds was performed by comparing the acquired mass spectra with those present in the NIST 2.0 Library, 2012 (National Institute of Standards

and Technology, Gaithersburg, MD, USA) database that accompanies the MassHunter Workstation-Qualitative Analysis software version B.06.00 Agilent Technologies (California, USA) in addition to comparing the retention index of the homologous series of *n*-alkanes C8-C30 (Supelco, 49451-U, Bellefonte, PA, USA) and with data from the literature.¹¹

Chemometric analysis

The acquisition data for the analysis obtained using the MassHunter Workstation software were processed on the MS-DIAL platform for deconvolution and alignment of the chromatograms. Furthermore, the metabolic profile data were organized in a spreadsheet (Excel, Microsoft),¹² where the identified compounds were arranged in columns and the sample names in rows, thus forming a data matrix.

The peak areas of the VOCs obtained via chromatograms were normalized by the sum treated on the cube root transformation scale that transform the response variable from y to $y^{1/3}$ and it was the type of transformation that provided a better normal distribution of the data obtained. Data were scaled according to the Pareto scale using the MetaboAnalyst 4.0 web base.¹³ In addition, multivariate chemometric analyses were performed, such as partial least squares-discriminant analysis (PLS-DA) and orthogonal projections to latent structures-discriminant analysis (OPLS-DA), beyond the construction of heat maps, hierarchical cluster analysis (HCA) graphs. Furthermore, multivariate ROC curves were generated through cross-validation to complement biomarker identification analyses, where two thirds (2/3) of the samples are used to assess the importance of the feature and the main features are then used to build classification models which are validated on 1/3 of the samples that were left out. The procedure was repeated several times to calculate the performance and confidence interval of each model. This entire procedure was also performed using the MetaboAnalyst 5.0 web base according to the protocol provided by Chong.¹⁴

Results

The pathogen

P. anacardii colonized the lower part of the mature cashew leaves (Figure S1, Supplementary Information (SI) section). From there, the fungus prevents the development of the leaves after penetrating the stomata and causing a reduction in the oxygen exchange between the plant and the environment.⁵ According to the field observations during the collecting months (March, April, May, June,

and July), the presence of the pathogen could be observed with different intensities. Between March and April, it was already possible to observe the presence of the fungus. However, there was no significant intensity when compared to May, when there was a severe infection, followed by a disease decline in June and July. These observations are in accordance with the literature, which reports that the first symptoms of the disease can be observed at the beginning of the rainy season, reaching its most serious point in May, coinciding with the end of the rainy season in Northeast Brazil.⁴

Profile of volatile organic compounds (VOCs)

Ninety-six compounds were tentatively identified from the four types of clones during the five months of analysis (Table S1, SI section). Most compounds belong to the terpene class. However, alcohols, esters, ketones, and aldehydes with short chains have also been identified. The results are in agreement with compounds already reported in the literature for the genus *Anacardium*, based on bibliographic research that takes into account family, genus, and species.¹⁵⁻²⁴ Thus, the confirmation by the literature that these compounds have already been identified in plants of the cashew tree genus, family, and species corroborates the fact that the compounds tentatively identified are products of plant biosynthesis and not of the fungus.

Data analysis

Owing to the amount and complexity of the data obtained, the results are presented as follows: metabolomic profile of each clone to verify the response of each clone along with the disease progress (March, April, and May) and decline (June and July). Comparisons were made between the profile of volatile organic compounds of clones resistant and susceptible to *P. anacardii*, aiming to verify which metabolites differ from the most resistant clones in relation to those susceptible clones; therefore, they could be biomarkers in response to pathogen attack.

Thus, the metabolic profiles of the clone BRS 226 (resistant to *P. anacardii*) were compared against the clones BRS 189 and CCP 76 (susceptible) as well as the comparison between BRS 265 (resistant) and the clones BRS 189 and CCP 76 was made on different models (PLS-DA and OPLS-DA). To check the accuracy and reliability of the model, the R^2Y and Q^2 parameters were used, called the explained variance, which provides a measure of fit of the model in relation to the original data, and the variable Q^2 , called the predicted variance, which provides the internal consistency of the measure between

the original and predictive data of the cross-validation (Table S2, SI section). Models with R^2Y and Q^2 values close to one were considered excellent. However, values above 0.5 are accepted when the sample components are highly complex. The closer these two parameters are to 1, the more stable and reliable the model.²⁵

In addition to the PLS-DA and OPLS-DA analyses, multivariate ROC curves were also constructed to identify possible biomarkers of resistance to black mold disease. As an important statistical tool, ROC curve graphs allow tests in which the rate of true positives (sensitivity) on the y-axis is plotted against the rate of false positives (specificity) on the x-axis. From this graph, it is possible to obtain the area under the curve (AUC). AUC is a measure of the accuracy of a diagnostic test, that is, a measure of the discriminatory ability of a test to verify whether a specific condition is present or absent.²⁶⁻²⁸ Assessing the usefulness of a biomarker identified by ROC curve tests based on its AUC can be done so that values between 0.9-1.0 are considered excellent. Already between 0.8-0.9 are classified as good; 0.7-0.8 are regular; 0.6-0.7 consider themselves poor; 0.5-0.6 indicates the test has no diagnostic value.²⁹ For this study, all curves constructed with a model 3 (with ten features) display a good performance and proved to be excellent in predicting compounds that may be candidates for biomarkers of resistance to black mold disease.

Analysis of the profile of volatile organic compounds of clone BRS 226 (resistant to *P. anacardii*) during the months of infestation and non-infestation

Discriminant analysis by partial least squares score graph (PLS-DA) (Figure 1a) explained 60.6% of the total variance through the first two components and showed intersections between the metabolite profiles in March and April, suggesting a similar volatile pattern for the initial months of infection. Volatile similarity was also observed between May (peak severity) and June-July (declining severity). The PLS-DA loading graph (Figure 1b) showed that (*E*)-hex-2-enal (**2**), (*Z*)-hex-3-en-1-ol (**3**), (*Z*)-hex-2-en-1-ol (**4**), (*E*)-hex-2-en-1-ol (**5**), hexan-1-ol (**6**), β -pinene (**15**), and oct-1-en-3-ol (**16**) may be associated with the differentiation between samples in May, June, and July, with the first two months of analysis (March and April). In contrast, camphene (**12**), α -fenchene (**13**), octan-3-one (**18**), limonene (**24**), β -*cis*-ocimene (**27**), and *p*-mentha-3,8-diene (**30**) may be associated with the differentiation in the profile of volatile compounds in March and April concerning the others.

The variable importance in the projection (VIP) graphs show the most relevant metabolites in the response

model with values above 1.0. The VIP graph (Figure 1c) constructed with data referring to samples from the BRS 226 clone over the months of March to July highlights that the most important compounds in the projection for the month of May include (*E*)-hex-2-enal (**2**), (*Z*)-hex-2-en-1-ol (**4**), hexan-1-ol (**6**), and α -phellandrene (**20**), which were reported in the literature for Anacardiaceae,^{30,31} a fact that corroborates that such compounds are plant biosynthesis products. These compounds can be considered as potential candidates for defense biomarkers of this clone against *P. anacardii*, considering that, in May, the severity of the pathogen in the field was observed with greater intensity in relation to the other months.

The heatmap graph (Figure S2, SI section) shows that compounds (*E*)-hex-2-enal (**2**), (*Z*)-hex-3-en-1-ol (**3**), (*Z*)-hex-2-en-1-ol (**4**), (*E*)-hex-2-en-1-ol (**5**), hexan-1-ol (**6**), β -pinene (**15**), and oct-1-en-3-ol (**16**)²⁴ showed a more pronounced increase in concentration in May, corroborating the data already pointed out by the VIP.

Comparative analysis of the volatile compound profiles of clones BRS 226 (resistant to *P. anacardii*) vs. BRS 189 (susceptible to *P. anacardii*)

The analysis for the behavior of the BRS 226 (resistant) and BRS 189 (susceptible), from March to July show, through the HCA graph (Figure S3a, SI section), that the volatile profiles are distinct for both clones (two groups). Within the large group of clone BRS 226, samples from March and April were grouped based on similarities in the metabolite profile, and samples from May, June, and July formed another group. The same pattern was observed for clone BRS 189. Thus, it is inferred that the samples have a similar chemical profile when the first signs of the pathogen are verified in the field. During the month of greatest severity, the metabolite profile changes in response to the stress to which the plants are subjected.

The PLS-DA (Figure S3b, SI section) score graph shows that most samples of the BRS 226 clone are found in the positive part of component 2, while the BRS 189 samples occupy the negative part of this component. It is still possible to verify that the differentiation in the profile of volatile compounds of the resistant clone (BRS 226) begins as early as March. All samples, except for July were found in the negative part of component 1. For the BRS 189 clone, there was significant differentiation in the volatile profile from April, since the samples from that month onwards are in the positive part of component 1. PLS-DA loading (Figure S3c, SI section) revealed that camphene (**12**), α -fenchene (**13**), β -myrcene (**17**), octan-3-one (**18**), pseudolimonene (**19**), limonene (**24**), sylvestrene (**26**), and

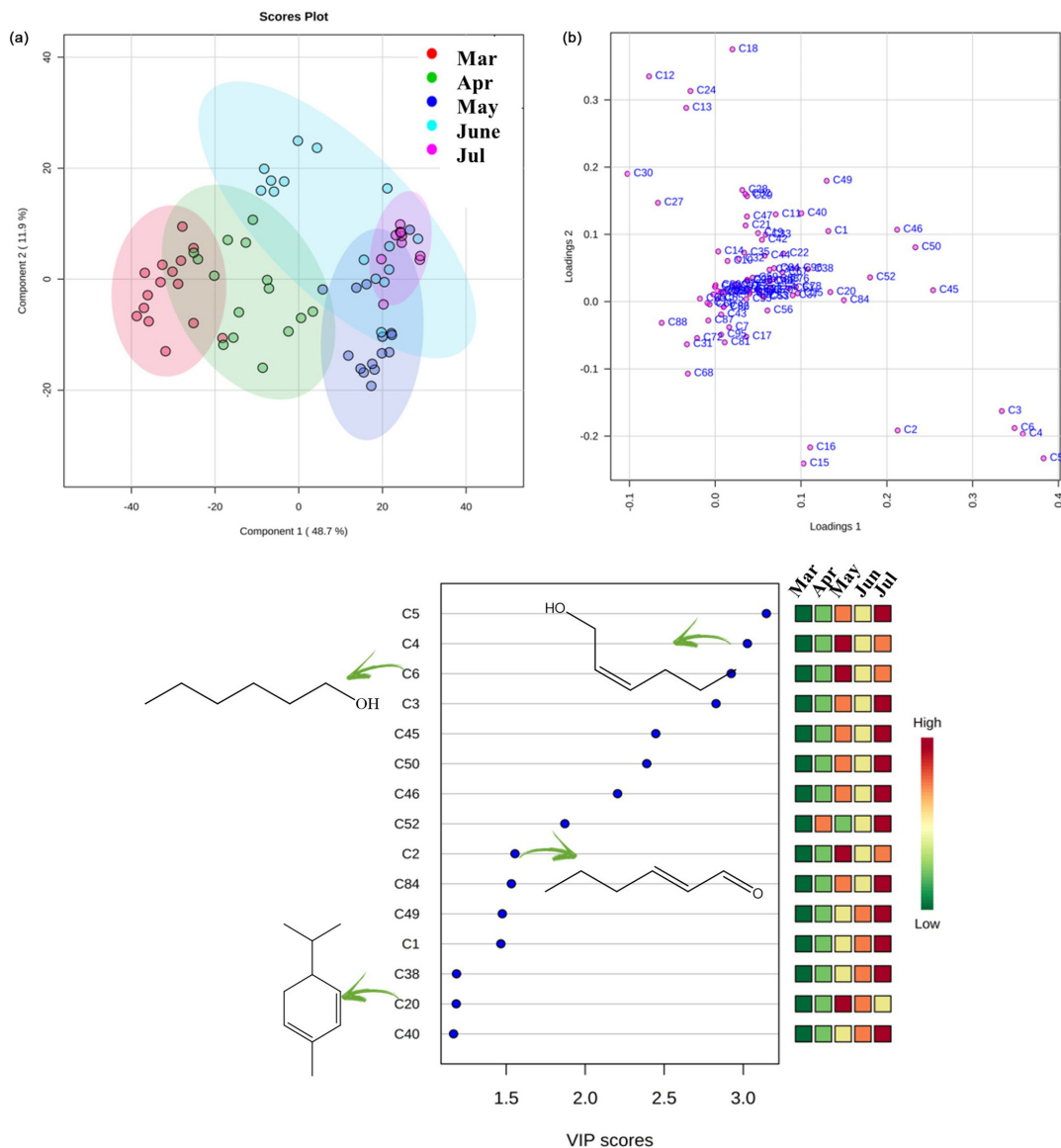


Figure 1. (a) Partial least squares discriminant analysis (PLS-DA) score and (b) loading, (c) graph of variables of importance in projection (VIP) built with the volatile compounds identified in the BRS 226 clone over May to July.

β -*cis*-ocimene (**27**)^{18,24,32} are VOCs related to discrimination between samples.

Using a supervised analysis tool, an orthogonal partial least squares discriminant analysis (OPLS-DA) graph was constructed with samples from clones BRS 226 and BRS 189 for May. This analysis was carried out to verify which VOCs were responsible for the differentiation between resistant and susceptible clones in the month of greatest disease severity.

The construction of the OPLS-DA score graph (Figure 2a) allowed us to verify the formation of two completely separate groups, which showed the different chemical responses of plants to the disease. The values of the quality parameters for the model were satisfactory: $R^2Y = 0.886$ and $Q^2 = 0.869$, suggesting that there was a

statistically significant difference between the metabolic profiles of the analyzed samples.

An S-plot dispersion graph (Figure 2b) was constructed to analyze the variables responsible for the separation between the groups observed in the OPLS-DA score graph. Discriminating compounds, that is, those at the ends of the graph axis and away from the center, common to both groups of samples, are highlighted by red circles. On the negative axis of the S-Plot are the compounds responsible for the discrimination of the susceptible clone (BRS 189), while on the positive axis there are the metabolites related to the resistant clone (BRS 226).

The VIP score graph (Figure 2c) corroborates the results obtained in the OPLS-DA S-Plot, which presents important antimicrobial VOCs already reported in the literature.³³

Thus, the biosynthesis of (*Z*)-hex-3-en-1-ol (**3**), (*Z*)-hex-2-en-1-ol (**4**), (*E*)-hex-2-en-1-ol (**5**), hexan-1-ol (**6**), oct-1-en-3-ol (**16**) and β -myrcene (**17**),^{18,23,34} present in the samples of the resistant clone in the month of greatest infestation (May), may participate as biomarkers in the defense mechanism of plants of BRS 226 clone.

The ROC curve (Figure 2d) constructed with the samples referring to both clones in the month of greatest infestation of *P. anacardii* in the field shows, through the AUC value, that the data provide a good diagnosis of which compounds contribute to the defense of the plants. The selection panel (Figure 2e) corroborates the compounds highlighted by the VIP graph as being identified in the samples of resistant clones (BRS 226) and also highlights the α -fenchene compound (**13**), a fact that reiterates that these compounds may be participating of the plant's defense mechanism and contributing to its greater resistance to the attack of the pathogen.

Comparative analysis of the volatile compound profiles of BRS 226 clones (resistant to *P. anacardii*) vs. CCP 76 (susceptible to *P. anacardii*)

The comparative analysis between the clones BRS 226 and CCP 76, resistant and susceptible, respectively, allows verification through HCA (Figure S4a, SI section) that the samples present a distinct volatile profile because the samples of the clones were separated into two large groups.

PLS-DA (Figure S4b, SI section) corroborates the separation of the HCA so that the samples referring to the BRS 226 clone are arranged on the positive part of component 2, whereas the samples from the CCP 76 clone are on the negative part of the same component. It is also worth mentioning that the samples referring to the BRS 226 clone are found, almost in their entirety (except for July), in the negative part of component 1. This shows that the defense compounds against pathogen attack were carried out in March when the presence of the fungus was first perceived. The CCP 76 clone, on the other hand, seems to initiate a change in metabolite biosynthesis only from April. Therefore, later when compared to BRS 226, a fact that may be associated with the susceptibility of this clone to the disease. The separation into two groups relative to each clone was confirmed by PLS-DA loading (Figure S4c, SI section), suggesting that camphene (**12**), α -fenchene (**13**), β -myrcene (**17**), and β -*cis*-ocimene (**27**)^{18,24} are discriminators between the two clones.

A OPLS-DA using data from May was performed to verify which metabolites were responsible for differentiating the samples from the resistant clone BRS

226 about the susceptible clone CCP 76 in the month of greatest disease severity. The OPLS-DA score graph (Figure 3a) suggests that plants have different chemical responses to infection by *P. anacardii*. The values of $R^2Y = 0.830$ and $Q^2 = 0.806$ were satisfactory, suggesting a statistically significant difference between the metabolic profiles of the samples analyzed.

Through the S-plot dispersion graph (Figure 3b), it was possible to identify the variables responsible for the separation between the groups observed in the OPLS-DA score graph. On the negative axis of the S-Plot are the compounds responsible for the discrimination of the resistant clone (BRS 226), while on the positive axis there are metabolites related to the susceptible clone (CCP 76).

β -Myrcene (**17**), sylvestrene (**26**), and myrtenol (**48**) were identified by VIP as the most abundant VOCs in the resistant clone in the month of May (Figure 3c), and were highlighted as candidates for resistance biomarkers of clone BRS 226, when compared with the susceptible clone CCP 76.

The construction of the ROC curve (Figure 3d) for the samples of the clones BRS 226 and CCP 76 shows good performance and, through Figure 3e, it can be seen that the compounds (*E,E*)-hexa-2,4-dienal (**9**), (*Z*)-butanoic acid, 3-hexenyl ester (**45**) in addition to myrtenol (**48**) are the ones that appear in greater abundance in the resistant clone in the period of greatest pathogen infestation in the field. Therefore, they can act in the defense mechanism of this plant, contributing to its greater resistance against *P. anacardii*.

Analysis of the profile of volatile organic compounds of clone BRS 265 (resistant to *P. anacardii*) during the months of infestation and non-infestation

The PLS-DA graph for BRS 265 clone revealed a separation between the samples over the five months of analysis (Figure 4a), and showed the difference in the profile of VOCs of the clone according to the presence or absence of disease. The PLS-DA loading graph (Figure 4b) showed that the compounds (*E*)-hex-2-enal, (**2**), (*Z*)-hex-3-en-1-ol (**3**), (*Z*)-hex-2-en-1-ol (**4**), (*E*)-hex-2-en-1-ol (**5**), hexan-1-ol (**6**), α -pinene (**11**), β -*cis*-ocimene (**27**), and β -*trans*-ocimene (**28**) were responsible for the separation of the samples according to the different months of analysis.

Compounds present in the VIP (Figure 4c) include those already reported in the literature for cashews, such as (*E*)-hex-2-enal, (**2**), α -pinene (**11**), β -*cis*-ocimene (**27**), α -copaene (**54**), γ -muurolene (**78**), and valencene (**84**),²³ with high concentrations in May and a decrease in June and July; therefore, they are potential response biomarkers to

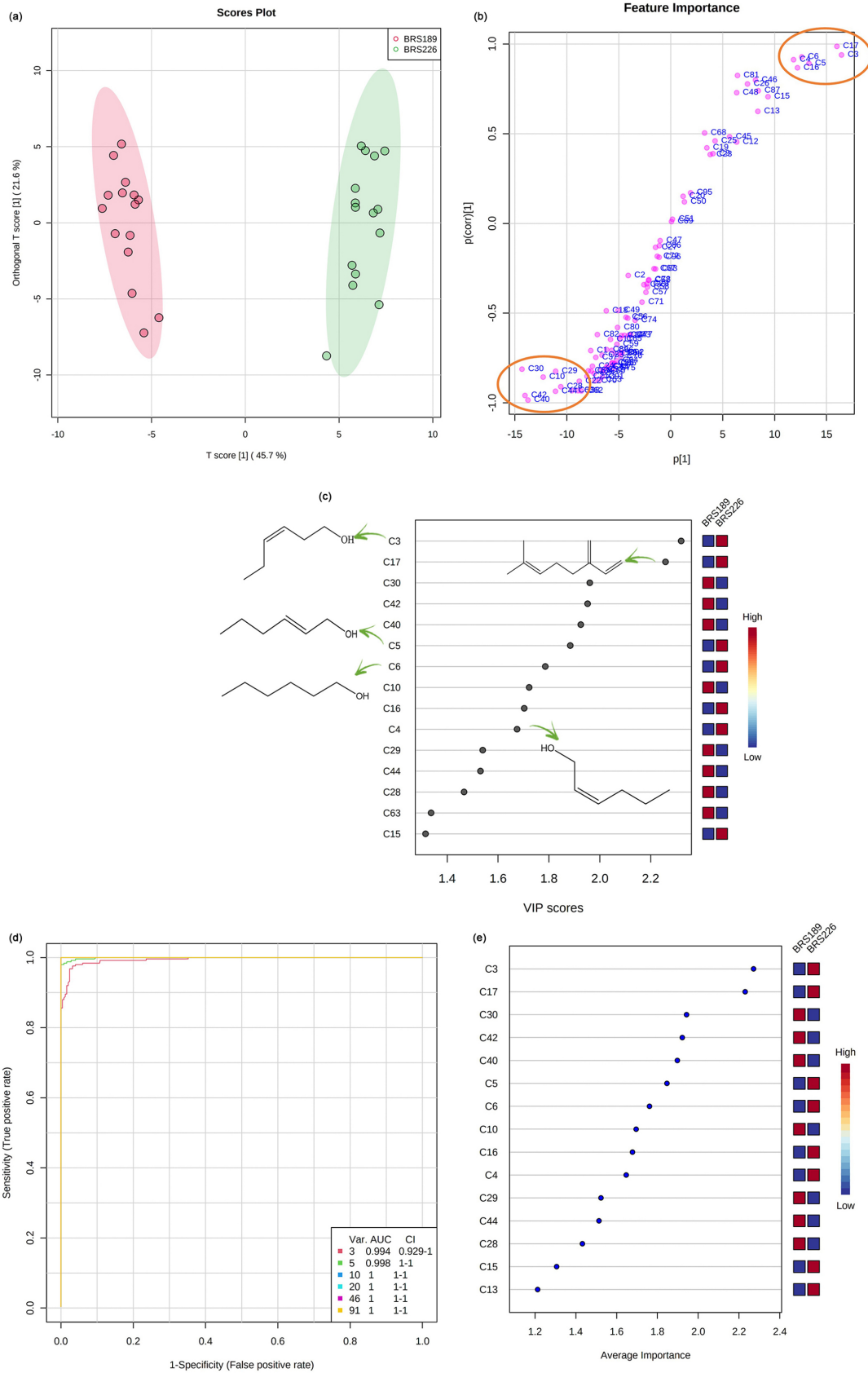


Figure 2. Graphs obtained from comparative analysis data between clones BRS 226 (resistant to *P. anacardii*) and BRS 189 (susceptible to *P. anacardii*) during May 2019: (a) OPLS-DA score; (b) S-Plot; (c) VIP score; (d) ROC curves for all models; (e) metabolites ranked by their selection importance in the ten-feature panel of model 3.

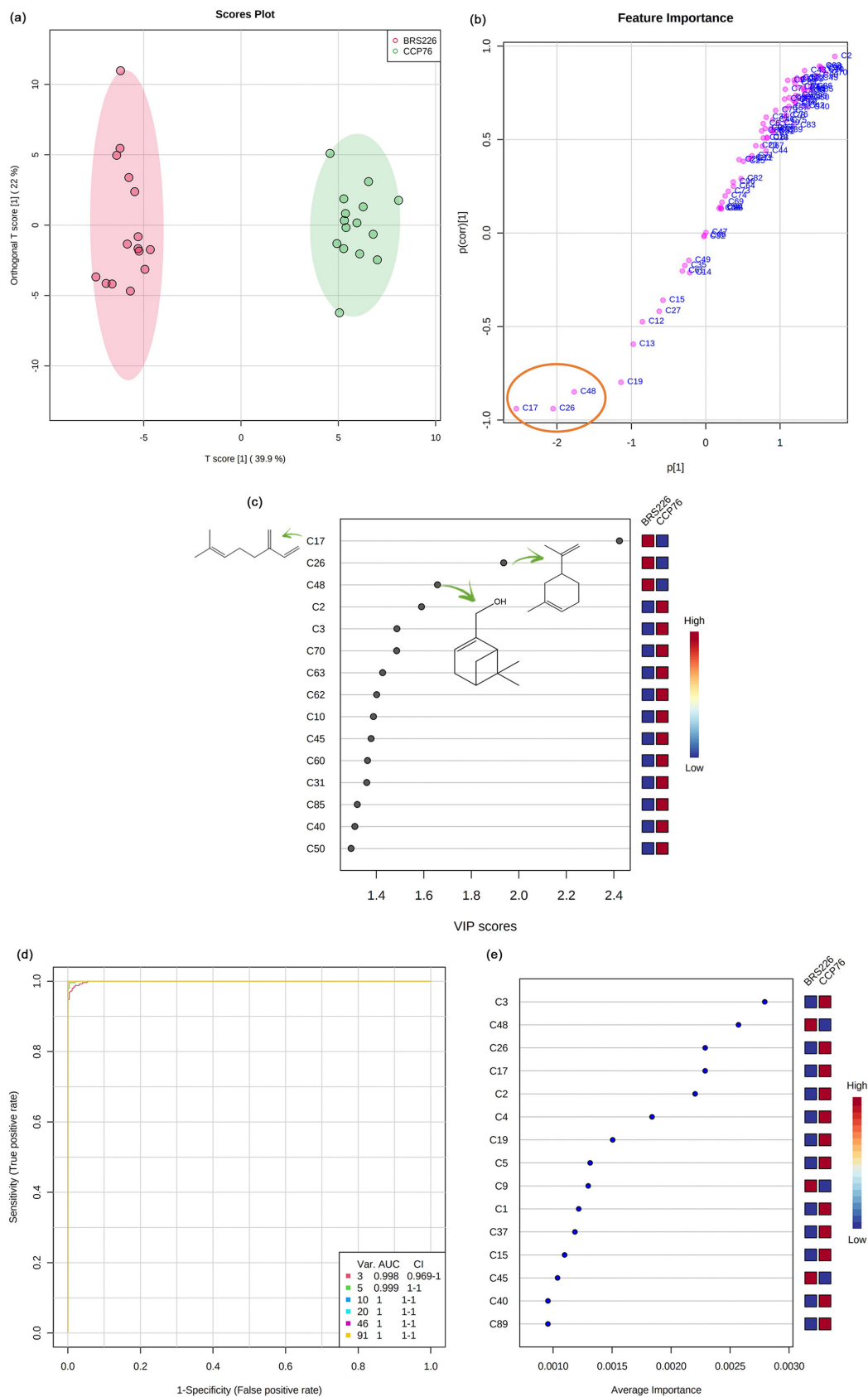


Figure 3. Graphs obtained from comparative analysis data between clones BRS 226 (resistant to *P. anacardii*) and CCP 76 (susceptible to *P. anacardii*) during May 2019: (a) OPLS-DA score; (b) S-Plot; (c) VIP score; (d) ROC curves for all models; (e) metabolites ranked by their selection importance in the ten-feature panel of model 3.

results obtained in the HCA regarding the segregation of the samples, and it is possible to verify that samples from BRS 189 are located in the negative quadrant of component 2. The samples from clone BRS 265 are in the positive quadrant of the same component. The PLS-DA loading graph (Figure S6c, SI section) shows the influence of variables on the samples and highlights some metabolites that were responsible for separating the groups over the months, being (*Z*)-hex-3-en-1-ol (**3**), (*Z*)-hex-2-en-1-ol (**4**), (*E*)-hex-2-en-1-ol (**5**), and (*Z*)-butanoic acid, 3-hexenyl ester (**45**)^{23,24} the main discriminants of the resistant clone samples (BRS 265) in relation to the susceptible one (BRS 189).

The volatile metabolite profiles for May of both clones were compared to identify candidate biomarkers for resistance to *P. anacardii*. The OPLS-DA score graph (Figure 5a) explains 51.2% of the total variance and suggests that the clones behave differently in terms of biosynthesis and emission of volatile organic compounds in response to infection by *P. anacardii*. The values of the quality parameters for the models $R^2Y = 0.930$ and $Q^2 = 0.911$ suggest that there is a statistically significant difference between the metabolic profiles of the samples.

The S-plot dispersion graph (Figure 5b) shows, on the negative axis, the compounds responsible for the discrimination of the susceptible clone (BRS 189), while on the positive axis there are the metabolites related to the resistant clone (BRS 265), all highlighted by a red circle.

The VIP score (Figure 5c) contains molecules already reported in the literature with antimicrobial activity,^{34,35} such as α -pinene (**11**), 1-octen-3-ol (**16**), β -*cis*-ocimene (**27**), chrysantenone (**36**), methyl salicylate (**47**), and α -copaene (**54**), which were more abundant in the samples of the resistant clone in May, corroborating the data presented by the S-Plot analysis. Thus, these compounds are highlighted as candidates for resistance biomarkers of the BRS 265 clone when compared with the susceptible BRS 189 clone.

The construction of the ROC curve (Figure 5d) allowed corroborating the presence of the compounds α -pinene (**11**), β -*cis*-ocimene (**27**), chrysantenone (**36**), and α -copaene (**54**) (Figure 5e) already highlighted by the VIP in the pathogen-resistant clone. In addition to confirming these compounds, *p*-mentha-3,8-diene (**30**), (4*E*,6*Z*)-allo-ocimene (**38**), (*E,E*)-2,4,6-octatriene, 2,6-dimethyl (**40**), and 2-hexenyl butyrate (**42**) are also highlighted.

Comparative analysis of the volatile compound profiles of BRS 265 clones (resistant to *P. anacardii*) vs. CCP 76 (susceptible to *P. anacardii*)

The HCA results (Figure S7a, SI section) showed

differences between the profiles of VOCs emitted by the two clones over the five months of analysis because it was possible to observe the clear separation of samples from both clones into two large groups from March to July.

The PLS-DA score (Figure S7b, SI section) confirmed the separation observed in the HCA. In negative values of component 2, there are samples related to clone BRS 265, and in positive values of the same component, there are samples from CCP 76. The samples for March and April of both clones were found in the negative part of component 1. However, the samples for May, June, and July are located in the positive part of component 1. This fact shows that an increase in the disease severity leads to a similar volatile pattern, indicating the biosynthesis of metabolites that can defend them from the attack of the pathogen. The PLS-DA loading graph (Figure S7c, SI section) highlights that the discrimination biomarkers include *neo-allo*-ocimene (**40**), (*E*)-butanoic acid, (*Z*)-2-hexenyl butyrate (**42**)^{23,24} for the CCP 76 clone and, in relation to BRS 265, the compounds β -myrcene (**17**), and chrysantenone (**36**).

OPLS-DA models were built to identify VOCs responsible for the differentiation of both clones in May. The OPLS-DA score graph (Figure 6a) explains 46.7% of the total variance and shows that the clones behave differently in the biosynthesis and emission of metabolites in response to black mold. The values of the quality parameters for the model were satisfactory: $R^2Y = 0.976$ and $Q^2 = 0.961$, suggesting that there was a statistically significant difference between the metabolic profiles of the samples analyzed.

The S-plot dispersion graph (Figure 6b) shows which variables were responsible for the separation between the groups observed in the score graph. The compounds responsible for the discrimination of the resistant clone (BRS 265) are located on the negative axis, while on the positive axis there are metabolites related to the susceptible clone (CCP 76).

The VIP score (Figure 6c) corroborate the results obtained in the OPLS-DA S-Plot, which presents VOCs already reported in the literature with antimicrobial activity.³⁹⁻⁴³ Terpenes and esters derivatives, such as α -pinene (**11**), pseudolimonene (**19**), sylvestrene (**26**), β -*cis*-ocimene (**27**), methyl salicylate (**47**), *cis*-3-hexenyl isovalerate (**49**), α -copaene (**54**), acoradien (**73**), germacrene D (**80**) and germacrene B (**96**) were the most abundant in the samples of the resistant clone BRS 265 in May and were highlighted as biomarkers candidates for its resistance of the BRS 265 clone when compared with the susceptible clone (CCP 76).

Through the analysis of the ROC curve (Figure 6d) it is possible to corroborate the compounds highlighted by the analysis of VIP scores, and the compounds (*E*)-hex-2-en-

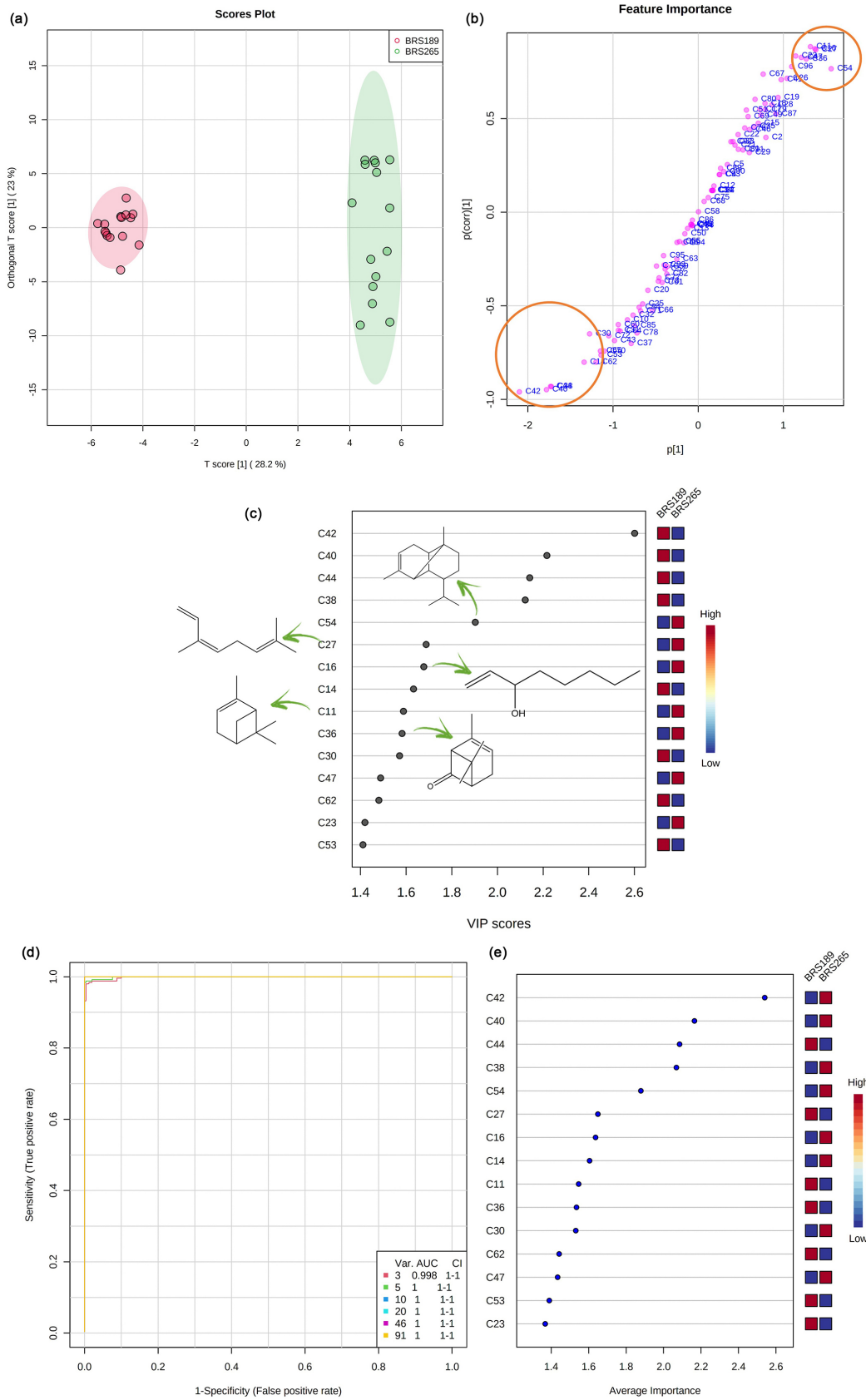


Figure 5. Graphs obtained from comparative analysis data between clones BRS 265 (resistant to *P. anacardii*) and BRS 189 (susceptible to *P. anacardii*) during May 2019: (a) OPLS-DA score; (b) S-Plot; (c) VIP score; (d) ROC curves for all models; (e) metabolites ranked by their selection importance in the ten-feature panel of model 3.

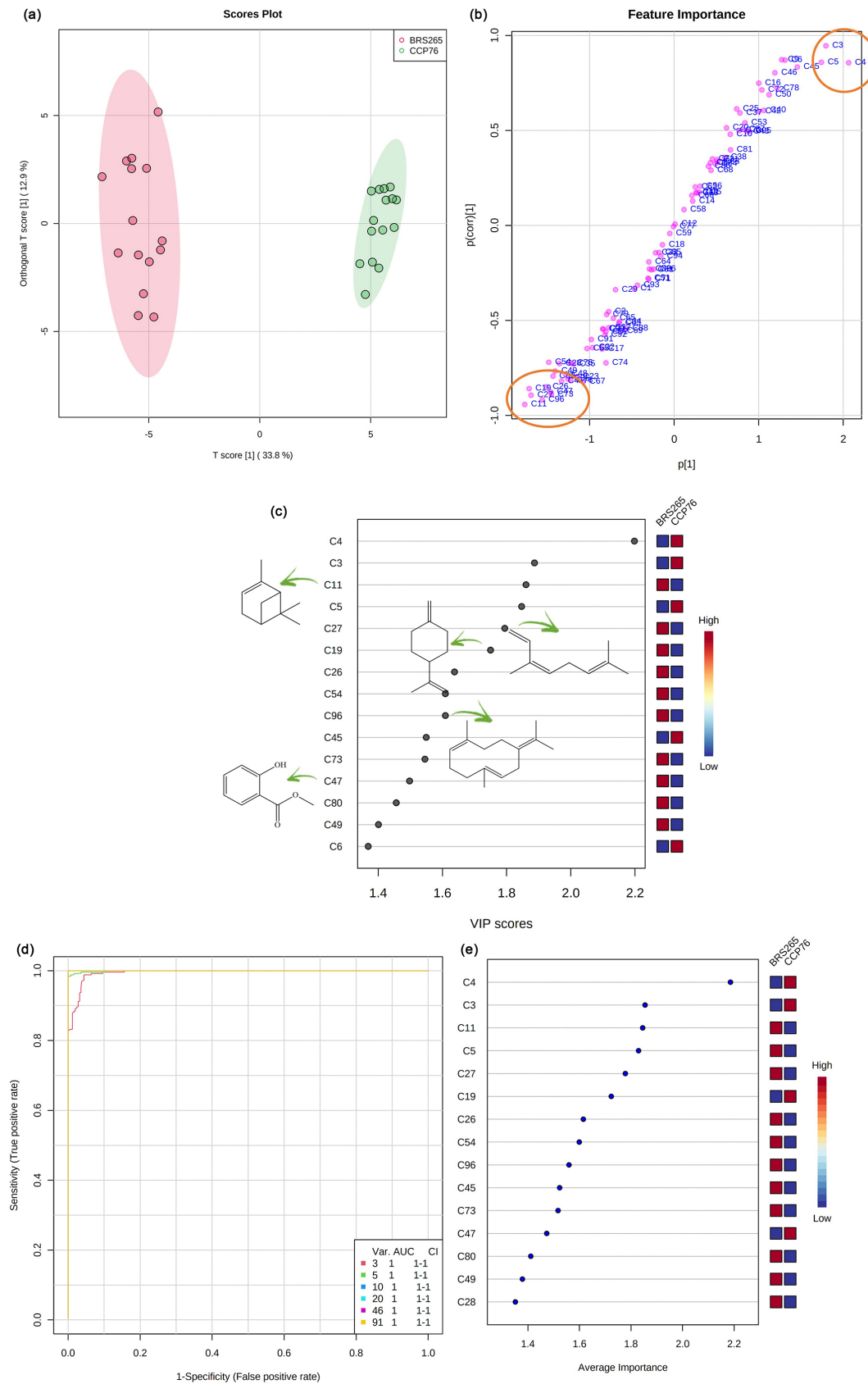


Figure 6. Graphs obtained from comparative analysis data between clones BRS 265 (resistant to *P. anacardii*) and CCP 76 (susceptible to *P. anacardii*) during May 2019: (a) OPLS-DA score; (b) S-Plot; (c) VIP score; (d) ROC curves for all models; (e) metabolites ranked by their selection importance in the ten- feature panel of model 3.

1-ol (**5**), β -*trans*-ocimene (**28**), (*Z*)-butanoic acid, 3-hexenyl ester (**45**) and acoradien (**73**) as present in samples from the resistant clone compared to the susceptible clone (Figure 6e).

Analysis of the profile of volatile compounds from the BRS 189 clone (susceptible to *P. anacardii*) during the months of infestation and non-infestation

The PLS-DA graph (Figure 7a) shows differences in the profile of VOCs emitted by the leaves of the BRS 189 clone in each month of analysis. Samples related to May formed a group that hardly intercepted the sample groups from other months. This fact is interesting when correlated with the observations made in the field, since in May, the plants were under conditions of greater infestation of the pathogen; therefore, their metabolic response tends to be different, aiming at their defense against biotic stress.

On the other hand, the sample groups in March and April showed a cross between each other, suggesting some similarity in the metabolic profile in these months. In addition, according to observations made in the field in March and April, the presence of the pathogen was already observed but without much severity, with the beginning of the infection attributed to that period. In June, there was a sharp drop in disease severity, so the profile of the metabolites was similar, in part, to that observed in July, when there were milder symptoms.

The PLS-DA loading graph (Figure 7b) suggests that VOCs are responsible for separating samples into groups, including (*Z*)-hex-3-en-1-ol (**3**), (*Z*)-hex-2-en-1-ol (**4**), (*E*)-hex-2-en-1-ol (**5**), hexan-1-ol (**6**), oct-1-en-3-ol (**16**), and guaia-1(10),11-diene (**87**), all of which have already been reported in the literature for the species *occidentale*.²⁴

According to the VIP (Figure 7c), 3-octanone (**18**), (4*E*,6*Z*)-*allo*-ocimene (**38**), *cis*-pinocampnone (**44**), and

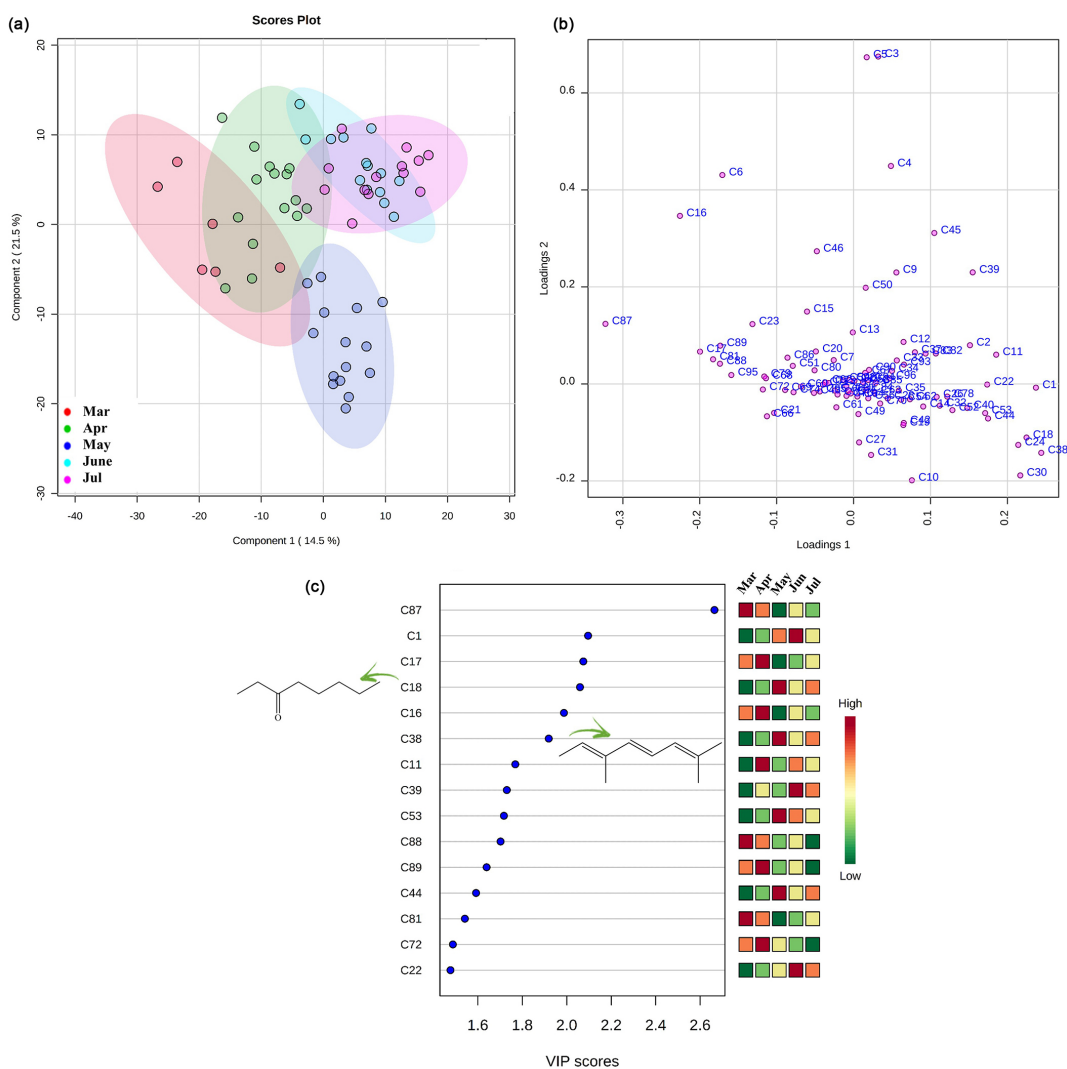


Figure 7. (a) Partial least squares discriminant analysis (PLS-DA) score and (b) loading, and (c) graph of variables of importance in projection (VIP) constructed with the volatile compounds identified in the BRS 189 clone from March to July.

α -ylangene (**53**)²³ contributed the most to the description of variables in May.

The heatmap (Figure S8, SI section) constructed based on the Euclidean distance measurement with the profile of volatile metabolites biosynthesized from March to July by the BRS 189 clone showed that there are differences in the plant metabolome according to the presence and absence of the pathogen. The metabolites α -thujene (**10**), octan-3-one (**18**), and terpinolene (**31**)^{24,44-46} showed a significant increase in concentration in May, which coincides with the period of increase in the severity of the disease in the field.

Analysis of the volatile compound profile of the CCP 76 clone (susceptible to *P. anacardii*) during months of infestation and non-infestation

The discrimination between the samples of the CCP 76 clone over the months of analysis was verified through the

construction of a PLS-DA score graph (Figure 8a). PLS-DA loading (Figure 8b) showed that separation of the monthly profiles occurred because of the presence of (*E*)-hex-2-enal (**2**), (*Z*)-hex-3-en-1-ol (**3**), (*Z*)-hex-2-en-1-ol (**4**), (*E*)-hex-2-en-1-ol (**5**), hexan-1-ol (**6**), (*E,E*)-2,4-hexadienal (**9**), α -thujene (**10**), α -pinene (**11**), oct-1-en-3-ol (**16**), octan-3-one (**18**), α -phellandrene (**20**), *o*-cymene (**25**), (*Z*)-butanoic acid, 3-hexenyl ester (**45**), α -terpineol (**46**), and *cis*-3-hexenyl valerate (**50**).

The VIP (Figure 8c) highlights that (*Z*)-hex-3-en-1-ol (**3**), octan-3-one (**18**), α -felandrene (**20**), and valencene (**84**)^{24,47} had higher concentrations in May, suggesting a relationship with a plant defense mechanism in the face of most diseases.

The heatmap (Figure S9, SI section) shows that compounds (*E*)-hex-2-enal (**2**), (*Z*)-hex-3-en-1-ol (**3**), (*Z*)-hex-2-en-1-ol (**4**), (*E*)-hex-2-en-1-ol (**5**), hexan-1-ol (**6**), hex-4-en-1-ol (**7**), (*E,E*)-2,4-hexadienal (**9**), 1-octen-

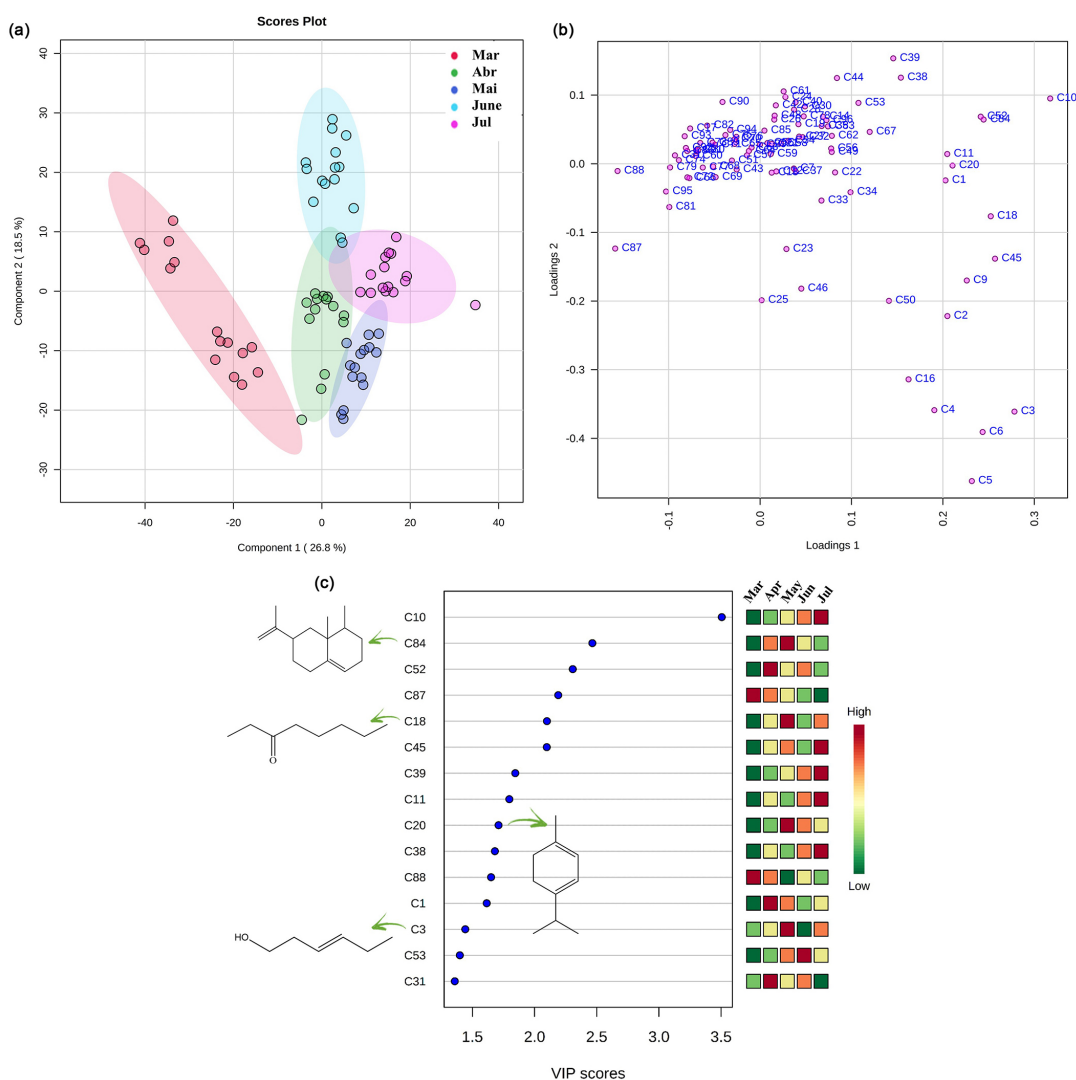


Figure 8. (a) Graphs of PLS-DA score, (b) loading, and (c) VIP score from the analyses during the months of March to July 2019 for the CCP 76 clone.

3-ol (**16**), octan-3-one (**18**), *o*-cymene (**25**), (*Z*)-butanoic acid, 3-hexenyl ester (**45**), α -terpineol (**46**), *cis*-valerate-3-hexenyl (**50**), and γ -muurolene (**78**) showed an increase in concentration in May. Many of these metabolites have been reported in the literature for the Anacardiaceae family.^{24,30,48,49}

The metabolites highlighted by the VIP and heatmap graphics can be associated with a plant defense system when the occurrence of the disease becomes more severe.⁵⁰ The compounds highlighted for the CCP 76 clone have already been reported in the literature for *A. occidentale*;^{17,20,23,25} therefore, they provide support for the fact that these compounds are products of the plant metabolism and not of the microorganism, and can therefore act together as a system of an attempt to defend plants against phytopathogen attack, especially in times of increased disease severity.

Discussion

The variety of VOCs emitted by plants is directly related to the environment to which they are subjected to biotic and abiotic stresses.⁵¹ They also act as the expression or silencing of defense genes. This allows plants to interact with each other under natural conditions in the field.⁵² Interactions between VOCs can potentiate the antimicrobial effects of the compounds when analyzed individually through a process of synergism.⁵³

VOCs commonly exhibit antimicrobial activity due to the presence of various classes of compounds, such as terpenes, alcohols, acids, esters, aldehydes, ketones, amines, among others.⁵¹ The antimicrobial activity of the constituents of a complex set of volatile metabolites is generally not attributed to a specific compound, since the synergistic effect must be taken into account. Indeed, certain compounds can modulate the antimicrobial effects of others.⁵⁴ One of the mechanisms of action of essential oils as antimicrobial agents is the ability of their constituents to penetrate the cells of microorganisms through the cell membrane and inhibit the cell's functional properties.⁵⁵

Volatile compounds such as aldehydes, alcohols, and esters of the six carbon atoms biosynthesized by leaves from higher plants are known as green leaf volatiles (GLVs). They are reported in the literature as important compounds in the defense and signaling mechanisms of plants against attack by herbivores, bacteria, and phytopathogenic fungi, in addition to being involved in communication processes between plants.⁵⁶ Under normal conditions, plants biosynthesize these compounds; however, under stress conditions, including those caused by the presence of phytopathogens, this biosynthesis occurs more quickly.⁵⁷⁻⁵⁹

GLVs are biosynthesized through the enzymatic pathway of lipoxygenase (LOX), which relies on the performance of various enzymes that convert lipid substrates into defense molecules.⁶⁰ Figure S10 (SI section) illustrates this biosynthetic pathway for the production of C6 aldehydes and alcohols.⁶¹

It was possible to observe, for the samples referring to the plants of the clones resistant to *P. anacardii*, the biosynthesis of short-chain aldehydes and alcohols, especially in the month of the greatest occurrence of the pathogen in the field (May). Therefore, the metabolites highlighted by the VIP, heatmap graphics and confirmed by ROC curve analysis can be associated with the defense system of the host against the pathogen.⁵⁰

Short-chain aldehydes are present in low concentrations in healthy plant leaves. However, their concentration may increase when the plant is exposed to attack by herbivores, insects, and microorganisms such as fungi.⁵⁷ This fact justifies the increase in the concentration of these compounds in the samples of resistant clones (BRS 226 and BRS 265) during the period of infection. These compounds, which have remarkable antifungal activity, modulate plant defense responses, leading to the biosynthesis of phytoalexins. *n*-Hexanal and (*Z*)-3-hexenal are biosynthesized through the cleavage of 13-hydroperoxides from linoleic and linolenic acids catalyzed by hydroperoxide lyase (HPL), whereas (*Z*)-3-hexenal can easily be converted into its (*E*)-2-hexenal isomer, which also has antimicrobial activity.⁵⁷ The biosynthesis of these compounds by plants attacked by fungi is reported to be responsible for inducing greater resistance in the host in the face of attack by phytopathogens.⁶¹

The biosynthesis of C6 alcohols is related to the response of the plant in an attempt to prevent the entry of the pathogen into plant cells.^{62,63} The BRS 226 clone is reported in the literature to be less affected by *P. anacardi*,⁸ thus the biosynthesis of compounds (*Z*)-hex-3-en-1-ol (**3**), (*Z*)-hex-2-en-1-ol (**4**), (*E*)-hex-2-en-1-ol (**5**), and hexan-1-ol (**6**), observed, especially in May, corroborates the fact that the plants of this clone emit a chemical response in order to defend themselves against the attack of the fungus, which may contribute to confer resistance to the pathogen.

Regarding the antimicrobial activity of volatile compounds, it is necessary to highlight the importance of the effects that may arise from the interaction between them. These effects can be additive, antagonistic or synergistic and depend on the concentration and number of compounds emitted by the plant.⁵³ Thus, some compounds highlighted for the susceptible clones according to the VIP have reports of antimicrobial activity, however, the fact that the BRS 189 and CCP 76 clones are more affected by

P. anacardii than BRS 226 and BRS 265 clones may be due to the insufficient concentration of these compounds to guarantee the protection of the plants. Another possibility is the antagonistic effect provoked by the interaction of these emitted compounds; that is, the isolated compounds present activity; however, their mixture does not present significant activity.

Concerning the resistant clone, BRS 265, similar to what was observed for BRS 226, there was an increase in the biosynthesis of compounds such as hexanal (**1**), (*E*)-hex-2-enal, (**2**), hex-4-en-1-ol (**7**), can be associated with the defense mechanism of plants that do so in an attempt to prevent the microorganism from penetrating its cellular structure.⁶³

In addition to C6 aldehydes and alcohols, compounds that include terpenes, such as α -pinene, δ -3-carene, β -myrcene, methyl salicylate, β -*cis*-ocimene, terpinolene, and α -copaene, also stood out in the investigated samples of cashew clones resistant to *P. anacardii* and may therefore be biomarker candidates for resistance by these plants in black mold. Studies have reported that oils rich in these compounds show significant antifungal activity.⁶⁴

Terpenes are compounds that are biosynthesized by plants and have various functions, such as attracting pollinators and herbivore predators, in addition to being responsible for the defense response of plants against phytopathogens, highlighting, in this aspect, monoterpenes.⁶⁵ In which many isoprenoids can be biosynthesized from damaged tissues through the activation of defense genes, aiming to protect the plant from the penetration of the pathogen in its cells.^{52,66,67} The variety and concentration of terpenes are decisive factors for the success of the antimicrobial activity of a set of volatile compounds emitted by plants.⁶⁷ Thus, the effects that the interaction between the compounds can cause, which can be additive, antagonistic, or synergistic, must be considered.³³

The diversity in the structure of monoterpenes is related to the types of cations that are produced during the process of biosynthesis of these compounds from geranyl pyrophosphate (GPP) and linalyl pyrophosphate (LPP) and neryl pyrophosphate (NPP) isomers.⁶⁸ Monoterpenes can be cyclic or acyclic, whereas monoterpenoids originate through biochemical reactions that give them the functions of esters, alcohols, ethers, aldehydes, and ketones. The monoterpene precursors are isopentenyl diphosphate (IPP) and its allylic isomer dimethylallyl diphosphate (DMAPP). The two possible biosynthetic pathways for the synthesis of IPP and DMAPP are the methyl-erythritol-4-phosphate (MEP) and acetate-mevalonate (MVA) pathways.^{66,68,69}

The biosynthesis of cyclic monoterpenes such as α -pinene occurs through the formation of a linear acyclic

intermediate from the isomerization of the initial geranyl diphosphate cation. Cycling produces an α -terpinyl cation, which undergoes secondary cycling. The biosynthesis of acyclic monoterpenes, such as myrcene and β -*cis*-ocimene, also involves isomerization of the geranyl diphosphate cation, but without cyclization processes (Figure S11, SI section).^{66,67}

Thus, the monoterpenes highlighted at higher concentrations in the samples of resistant clones contribute to the defense of these plants against the fungus that causes black mold.

Conclusions

In this study, it was possible to observe different behaviors of VOC biosynthesis in dwarf cashew clones according to the stress caused by *P. anacardii* infestations. BRS 265 and BRS 226 showed resistance to *P. anacardii* in the analyzed periods. Chemometric analyzes for spectral data of BRS 265 allowed to identify (*E*)-hex-2-enal (**2**), α -pinene (**11**), pseudolimonene (**19**), sylvestrene (**26**), β -*cis*-ocimene (**27**), methyl salicylate (**47**), α -copaene (**54**), γ -muurolene (**78**), germacrene D (**80**), valencene (**84**), and germacrene B (**96**) as VOCs associated with its defense mechanism. On the other hand, (*E*)-hex-2-enal (**2**), (*Z*)-hex-3-en-1-ol (**3**), (*Z*)-hex-2-en-1-ol, (**4**), (*Z*)-hex-2-en-1-ol (**5**), hexan-1-ol (**6**), β -myrcene (**17**), α -phellandrene (**20**), sylvestrene (**26**), and myrtenol (**48**) are for clone BRS 226. The chemometric data also made it possible to verify that the metabolite profile of susceptible clones were similar and the compounds octan-3-one (**18**), (4*E*,6*Z*)-allo-ocimene (**38**), *cis*-pinocamphone (**44**) and α -ylangene (**53**) for clone BRS 189 and (*Z*)-hex-3-en-1-ol (**3**), octan-3-one (**18**), α -phellandrene (**20**), butanoic acid, 3-hexenyl ester, (*Z*)- (**51**) and valencene (**84**) for CCP 76 can be biomarkers of the presence of the pathogen. These findings suggested some VOCs involved in the host's attempt to combat the pathogen *P. anacardii* and provided an important step to carry out studies of the development of natural pesticides to protect orchards cashew trees.

Supplementary Information

Supplementary data (table about chemical composition of essential oil of dwarf cashew trees, table about multivariate analysis, figures about heatmaps analysis, HCAs analysis, PLS-DA analysis, figures about biosynthetic path following the LOX route for the production of green leaf volatiles and biosynthesis of acyclic and cyclic monoterpenes from geranyl diphosphate, chromatograms, and mass spectra) are available free of charge at <http://jbc.sbq.org.br> as PDF file.

Acknowledgments

The authors gratefully acknowledge the financial support from the National Council for Scientific and Technological Development (CNPq, Conselho Nacional de Desenvolvimento Científico e Tecnológico), National Institute of Science and Technology - INCT BioNat, grant No. 465637/2014-0, Brazil, and the Coordination for the Improvement of Higher Education Personnel (Coordenação de Aperfeiçoamento de Pessoal de Nível Superior - CAPES, Finance Code 001).

Author Contributions

Deborah B. de Sousa was responsible for methodology, formal analysis, investigation, resources, data curation, writing original draft; Gisele S. da Silva for investigation, writing review and editing; Jhonyson A. C. Guedes for investigation, writing review and editing; Luiz A. L. Serrano for conceptualization, investigation, writing review and editing; Marlon V. V. Martins for conceptualization, investigation, resources, writing review and editing; Tigressa H. S. Rodrigues for conceptualization, investigation, resources, writing review and editing; Edy S. de Brito for conceptualization, writing review and editing, supervision; Davila Zampieri for conceptualization, writing review and editing, supervision; Mary A. S. Lima for conceptualization, writing review and editing, supervision; Guilherme J. Zocolo for conceptualization, methodology, resources, writing review and editing, supervision, project administration, funding acquisition.

References

- Instituto Brasileiro de Geografia e Estatística (IBGE); *Levantamento Sistemático da Produção Agrícola*; Rio de Janeiro, 2017. [Link] accessed in May 2022
- Cavalcanti, J. J. V.; de Resende, M. D. V.; *Rev. Bras. Frutic.* **2010**, *32*, 1279. [Crossref]
- Mycobank Database, <http://www.mycobank.org/Biolomics.aspx?Table=Mycobank&Rec=279264&Fields=All>, accessed in May 2022.
- Freire, F. C. O.; Cardoso, J. E.; dos Santos, A. A.; Viana, F. M. P.; *Crop Prot.* **2002**, *21*, 489. [Crossref]
- Viana, F. M. P.; Lima, J. S.; Lima, F. A.; Cardoso, J. E.; *Tropical Plant Pathology* **2012**, *37*, 354. [Crossref]
- López-Gresa, M. P.; Lisón, P.; Campos, L.; Rodrigo, I.; Rambla, J. L.; Granell, A.; Conejero, V.; Bellés, J. M.; *Front. Plant Sci.* **2018**, *8*, 1855. [Crossref]
- Mhlongo, M. I.; Piater, L. A.; Madala, N. E.; Labuschagne, N.; Dubery, I. A.; *Front. Plant Sci.* **2018**, *9*, 112. [Crossref]
- Lima, J. S.; Martins, M. V. V.; Serrano, L. A. L.; Vidal Neto, F. C.; Viana, F. M. P.; Cardoso, J. E.; *Reação de Clones de Cajueiro-anão à Antracnose e ao Mofo-preto*; Embrapa: Fortaleza, 2019. [Link] accessed in May 2022
- Serrano, L. A. L.; de Oliveira, V. H.; *Agronegócio Caju: Práticas e Inovações*, vol. 16; Embrapa, Ed.: Brasília, Brazil, 2013.
- Rouseff, R. L.; Onagbola, E. O.; Smoot, J. M.; Stelinski, L. L.; *J. Agric. Food Chem.* **2008**, *56*, 8905. [Crossref]
- Adams, R. P.; *Identification of Essential Oil Components by Gas Chromatography/Mass Spectroscopy*, 4.1th ed.; Carol Stream: Illinois, USA, 2017.
- Microsoft Office Excel*, version 365; Microsoft, USA, 2021.
- MetaboAnalyst 5.0, www.metaboanalyst.ca, accessed in May 2022.
- Chong, J.; Wishart, D. S.; Xia, J.; *Curr. Protoc. Bioinf.* **2019**, *68*, 1. [Crossref]
- Agila, A.; Barringer, S. A.; *J. Food Sci.* **2011**, *76*, C768. [Crossref]
- Bicalho, B.; Rezende, C. M.; *Z. Naturforsch. C* **2001**, *56*, 35. [Crossref]
- Ceva-Antunes, P. M. N.; Bizzo, H. R.; Silva, A. S.; Carvalho, C. P. S.; Antunes, O. A. C.; *LWT - Food Sci. Technol.* **2006**, *39*, 437. [Crossref]
- Dzamic, A.; Gbolade, A.; Ristic, M.; Marin, P. D.; *Chem. Nat. Compd.* **2009**, *45*, 441. [Crossref]
- Garruti, D. S.; Franco, M. R. B.; da Silva, M. A. A. P.; Janzanti, N. S.; Alves, G. L.; *J. Sci. Food Agric.* **2003**, *83*, 1455. [Crossref]
- Gebara, S. S.; Ferreira, W. O.; Ré-Poppi, N.; Simionatto, E.; Carasek, E.; *Food Chem. J.* **2011**, *127*, 689. [Crossref]
- Cardoso, C. A. L.; Jeller, A. H.; Ré-Poppi, N.; Coelho, R. M.; Yasunaka, D. S.; Schleder, E. J. D.; *J. Essent. Oil Res.* **2010**, *22*, 469. [Crossref]
- Ling, B.; Yang, X.; Li, R.; Wang, S.; *Eur. J. Lipid Sci. Technol.* **2016**, *118*, 1368. [Crossref]
- Liu, H.; An, K.; Su, S.; Yu, Y.; Wu, J.; Xiao, G.; Xu, Y.; *Foods* **2020**, *9*, 75. [Crossref]
- Salehi, B.; Gültekin-Özgüven, M.; Kirkin, C.; Özçelik, B.; Morais-Braga, M. F. B.; Carneiro, J. N. P.; Bezerra, C. F.; da Silva, T. G.; Coutinho, H. D. M.; Amina, B.; Armstrong, L.; Selamoglu, Z.; Sevindik, M.; Yousaf, Z.; Sharifi-Rad, J.; Muddathir, A. M.; Devkota, H. P.; Martorell, M.; Jugran, A. K.; Martins, N.; Cho, W. C.; *Biomolecules* **2019**, *9*, 465. [Crossref]
- Chagas-Paula, D. A.; Zhang, T.; da Costa, F. B.; Edrada-Ebel, R.; *Metabolites* **2015**, *5*, 404. [Crossref]
- Bünger, R.; Mallet, R. T.; *Crit. Care Med.* **2016**, *44*, 1784. [Crossref]
- Hoo, Z. H.; Candlish, J.; Teare, D.; *Emerg. Med. J.* **2017**, *34*, 357. [Crossref]
- Yu, Q.; Liu, X.; Huang, H.; Zheng, X.; Pan, X.; Fang, J.; Meng, L.; Zhou, C.; Zhang, X.; Li, Z.; Zou, D.; *Ther. Adv. Gastroenterol.* **2019**, *12*, 1. [Crossref]
- Xia, J.; Broadhurst, D. I.; Wilson, M.; Wishart, D. S.; *Metabolomics* **2013**, *9*, 280. [Crossref]

30. Maia, J. G. S.; Andrade, E. H. A.; Zoghbi, M. D. G. B.; *J. Food Compos. Anal.* **2000**, *13*, 227. [Crossref]
31. de Aquino, N. C.; Araújo, R. M.; Silveira, E. R.; *J. Braz. Chem. Soc.* **2017**, *28*, 907. [Crossref]
32. Zoghbi, M. G. B.; Pereira, R. A.; de Lima, G. S. L.; Bastos, M. N. C.; *Quim. Nova* **2014**, *37*, 1188. [Crossref]
33. Iijima, Y.; *Metabolites* **2014**, *4*, 699. [Crossref]
34. da Silva, A. C. R.; Lopes, P. M.; de Azevedo, M. M. B.; Costa, D. C. M.; Alviano, C. S.; Alviano, D. S.; *Molecules* **2012**, *17*, 6305. [Crossref]
35. Mneimne, M.; Baydoun, S.; Nemer, N.; Apostolides, N.; *Med. Aromat. Plants* **2016**, *5*, 5. [Crossref]
36. Perigo, C. V.; Torres, R. B.; Bernacci, L. C.; Guimarães, E. F.; Haber, L. L.; Facanali, R.; Vieira, M. A. R.; Quecini, V.; Marques, M. O. M.; *Ind. Crops Prod.* **2016**, *94*, 528. [Crossref]
37. Smeriglio, A.; Trombetta, D.; Cornara, L.; Valussi, M.; de Feo, V.; Caputo, L.; *Molecules* **2019**, *24*, 2941. [Crossref]
38. Brillì, F.; Loreto, F.; Baccelli, I.; *Front Plant Sci.* **2019**, *10*, 264. [Crossref]
39. Falahati, M.; Sepahvand, A.; Mahmoudvand, H.; Baharvand, P.; Jabbarnia, S.; Ghoghghi, A.; Yarahmadi, M.; *Curr. Med. Mycol.* **2015**, *1*, 25. [Crossref] [PDF]
40. Hristova, Y.; Wanner, J.; Jirovetz, L.; Stappen, I.; Iliev, I.; Gochev, V.; *Biotechnol. Biotechnol. Equip.* **2015**, *29*, 592. [Crossref]
41. Giweli, A.; Džamic, A. M.; Sokovic, M.; Ristic, M. S.; Marin, P. D.; *Molecules* **2012**, *17*, 4836. [Crossref]
42. Ismail, A.; Lamia, H.; Mohsen, H.; Samia, G.; Bassem, J.; *Sci. Int.* **2013**, *1*, 148. [Crossref] [PDF]
43. Kirchner, K.; Wisniewski, A.; Cruz, A. B.; Biavatti, M. W.; Netz, D. J. A.; *Rev. Bras. Farmacogn.* **2010**, *20*, 692. [Crossref]
44. Bortolucci, W. C.; de Oliveira, H. L. M.; Silva, E. S.; Boas, M. R. V.; de Carvalho, T. M.; Campo, C. F. A. A.; Gonçalves, J. E.; Júnior, R. P.; Gazim, Z. C.; *Aust. J. Crop Sci.* **2018**, *12*, 1645. [Crossref]
45. Montanari, R. M.; Barbosa, L. C. A.; Demuner, A. J.; Silva, C. J.; Andrade, N. J.; Ismail, F. M. D.; Barbosa, M. C. A.; *Molecules* **2012**, *17*, 9728. [Crossref]
46. Papageorgiou, V. P.; Assimopoulou, A. N.; Yannovits-Argiriadis, N.; *J. Essent. Oil Res.* **1999**, *11*, 367. [Crossref]
47. Kossouh, C.; Moudachirou, M.; Adjakidje, V.; Chalchat, J. C.; Figuéredo, G.; *J. Essent. Oil Res.* **2008**, *20*, 5. [Crossref]
48. Deveci, O.; Sukan, A.; Tuzun, N.; Kocabas, E. E. H.; *J. Med. Plants Res.* **2010**, *4*, 2211. [Crossref] [PDF]
49. Sosa-Moguel, O.; Pino, J. A.; Sauri-Duch, E.; Cuevas-Glory, L.; *Int. J. Food Prop.* **2018**, *21*, 1008. [Crossref]
50. Castro-Moretti, F. R.; Gentzel, I. N.; Mackey, D.; Alonso, A. P.; *Metabolites* **2020**, *10*, 52. [Crossref]
51. Calo, J. R.; Crandall, P. G.; O'Bryan, C. A.; Ricke, S. C.; *Food Control* **2015**, *54*, 111. [Crossref]
52. Kishimoto, K.; Matsui, K.; Ozawa, R.; Takabayashi, J.; *Plant Cell Physiol.* **2005**, *46*, 1093. [Crossref]
53. dos Santos, A. L.; Polidoro, A. S.; Cardoso, C. A. L.; Mota, J. S.; Jacques, R. A.; Caramão, E. B.; *J. Braz. Chem. Soc.* **2019**, *30*, 2691. [Crossref]
54. Russo, R.; Corasaniti, M. T.; Bagetta, G.; Morrone, L. A.; *J. Evidence-Based Complementary Altern. Med.* **2015**, *2015*, 397821. [Crossref]
55. Bajpai, V. K.; Baek, K. H.; Kang, S. C.; *Food Res. Int.* **2012**, *45*, 722. [Crossref]
56. Tanaka, T.; Ikeda, A.; Shiojiri, K.; Ozawa, R.; Shiki, K.; Nagai-Kunihiro, N.; Fujita, K.; Sugimoto, K.; Yamato, K. T.; Dohra, H.; Ohnishi, T.; Koeduka, T.; Matsui, K.; *Plant Physiol.* **2018**, *178*, 552. [Crossref]
57. Kishimoto, K.; Matsui, K.; Ozawa, R.; Takabayashi, J.; *Phytochemistry* **2008**, *69*, 2127. [Crossref]
58. Ameye, M.; Allmann, S.; Verwaeren, J.; Smagghe, G.; Haesaert, G.; Schuurink, R. C.; Audenaert, K.; *New Phytol.* **2018**, *220*, 666. [Crossref]
59. Ponzio, C.; Gols, R.; Pieterse, C. M. J.; Dicke, M.; *Funct. Ecol.* **2013**, *27*, 587. [Crossref]
60. Vincenti, S.; Mariani, M.; Alberti, J. C.; Jacopini, S.; de Caraffa, V. B. B.; Berti, L.; Maury, J.; *Catalysts* **2019**, *9*, 873. [Crossref]
61. ul Hassan, M. N.; Zainal, Z.; Ismail, I.; *Plant Biotechnol. J.* **2015**, *13*, 727. [Crossref]
62. López-Gresa, M. P.; Lisón, P.; Campos, L.; Rodrigo, I.; Rambla, J. L.; Granell, A.; Conejero, V.; Bellés, J. M.; *Front. Plant Sci.* **2017**, *8*, 1188. [Crossref]
63. Scala, A.; Allmann, S.; Mirabella, R.; Haring, M. A.; Schuurink, R. C.; *Int. J. Mol. Sci.* **2013**, *14*, 17781. [Crossref]
64. Powers, C. N.; Osier, J. L.; Mcfeeters, R. L.; Brazell, C. B.; Olsen, E. L.; Moriarity, D. M.; Satyal, P.; Setzer, W. N.; *Molecules* **2018**, *23*, 13. [Crossref]
65. Ramak, P.; Osaloo, S. K.; Sharifi, M.; Behmanesh, M.; *J. Med. Plants Res.* **2014**, *8*, 983. [Crossref]
66. Haque, E.; Irfan, S.; Kamil, M.; Sheikh, S.; Hasan, A.; Ahmad, A.; Lakshmi, V.; Nazir, A.; Mir, S. S.; *Microbiology (Moscow, Russ. Fed.)* **2016**, *85*, 436. [Crossref]
67. Mihai, A. L.; Popa, M. E.; *Agric. Agric. Sci. Procedia* **2015**, *6*, 585. [Crossref]
68. Dorta, E.; González, M.; Lobo, M. G.; Sánchez-Moreno, C.; de Ancos, B.; *Food Res. Int.* **2014**, *57*, 51. [Crossref]
69. Mahizan, N. A.; Yang, S.; Moo, C.-L.; Song, A. A.-L.; Chong, C.-M.; Chong, C.-W.; Abushelaibi, A.; Lim, S.-H. E.; Lai, K.-S.; *Molecules* **2019**, *24*, 2631. [Crossref]

Submitted: February 2, 2022

Published online: May 24, 2022

